Higgs enhancement for the dark matter relic density

Julia Harz*
Sorbonne Universités, Institut Lagrange de Paris (ILP), 98 bis Boulevard Arago, 75014 Paris, France and Laboratoire de Physique Théorique et Hautes Energies (LPTHE), UMR 7589 CNRS & UPMC, 4 Place Jussieu, F-75252 Paris, France

Kalliopi Petraki†
Laboratoire de Physique Théorique et Hautes Energies (LPTHE), UMR 7589 CNRS & UPMC, 4 Place Jussieu, F-75252 Paris, France and Nikhef, Science Park 105, 1098 XG Amsterdam, Netherlands

(Received 20 November 2017; published 30 April 2018)

We consider the long-range effect of the Higgs on the density of thermal-relic dark matter. While the electroweak gauge boson and gluon exchange have been previously studied, the Higgs is typically thought to mediate only contact interactions. We show that the Sommerfeld enhancement due to a 125 GeV Higgs can deplete TeV-scale dark matter significantly and describe how the interplay between the Higgs and other mediators influences this effect. We discuss the importance of the Higgs enhancement in the minimal supersymmetric standard model and its implications for experiments.

DOI: 10.1103/PhysRevD.97.075041

I. INTRODUCTION

The dark matter (DM) density has been determined to an unprecedented precision by the Planck satellite [1]:

$$\Omega_{\rm DM}h^2 = 0.1199 \pm 0.0022. \quad (1)$$

This measurement provides a powerful constraint on DM theories. However, in order to constrain DM models reliably, it is essential to compute the expected DM density in a comprehensive manner.

It is well known that the density of thermal-relic DM is determined by the strength of the DM annihilation processes. These include the DM self-annihilations, as well as the coannihilations of DM with particles of similar mass. The latter were first discussed in [2] but have received renewed attention recently, in particular in the context of DM coupled to the weak interactions of the standard model (SM), known as WIMP DM [3–10].

Moreover, it is well established that if DM or its coannihilating partners couple to significantly lighter force mediators, then nonperturbative effects—the Sommerfeld enhancement of the annihilation processes [11,12] and the formation of unstable bound states [13]—become important. It has been shown, in particular, that the electroweak gauge boson exchange, as well as the gluon exchange in the case of DM coannihilating with colored particles, can affect significantly the density of WIMP DM with mass as low as ∼500 GeV (see e.g. [14–18]). On the other hand, the Higgs exchange has been neglected so far, or studied only insufficiently [19]. The rationale has been twofold: The Higgs boson, being heavier, yields a shorter-range force than the SM gauge bosons, and the DM coupling to the Higgs is in many models smaller than, or only comparable to the SM gauge couplings.

In this work, we demonstrate that, contrary to the above expectation, the Higgs enhancement can be significant. We employ a simplified model in which DM coannihilates with colored particles that couple to a SM-like Higgs. While this setup has wider applicability, it is inspired by the minimal supersymmetric SM (MSSM) and the measurement of the Higgs mass, which together motivate light stops with large coupling to the Higgs [20,21]. Related DM studies in the MSSM have been conducted recently [10,22,23]. Moreover, this setup allows us to directly compare the effect of the Higgs exchange with that of other mediators, in particular the gluons. As we show, the Higgs enhancement is significant even for moderate couplings to the Higgs, and can be comparable to the gluon exchange.

This letter is organized as follows: After specifying the simplified model, we review the DM freeze-out in the presence of coannihilations. We describe the effect of the Higgs enhancement on the annihilation cross section before demonstrating its impact on the DM abundance. We

*jharz@lpthe.jussieu.fr
†kpetraki@lpthe.jussieu.fr

conclude with a discussion of the Higgs enhancement in the MSSM and its experimental implications.

II. SIMPLIFIED MODEL

We assume that DM is a Majorana fermion χ of mass m_χ, that coannihilates with a complex scalar X of mass m_X. χ and X are the lightest and next-to-lightest particles (LP and NLP) odd under a $\mathbb{Z}_2$ symmetry that prevents the LP from decaying. For our purposes, we need not specify the χ interactions with X or other particles further. X transforms as a **3** under $SU(3)_c$, and couples to a real scalar h of mass $m_h = 125$ GeV, via

$$\delta\mathcal{L} = (D_{\mu,ij}X_j)^\dagger(D^\mu_{ij'}X_{j'}) - m_X^2 X_j^\dagger X_j + \frac{1}{2}(\partial_\mu h)(\partial^\mu h) - \frac{1}{2}m_h^2 h^2 - g_h m_X h X_j^\dagger X_j. \quad (2)$$

Here, $D_{\mu,ij} = \delta_{ij}\partial_\mu - ig_s G^a_\mu T^a_{ij}$, with G^a_μ being the gluon fields and T^a the corresponding generators. In a complete model, the scalar potential includes also the quartic terms. Moreover, a SM-like Higgs would couple to the SM particles. For simplicity, we do not consider these couplings, whose effect is well known. We focus instead on the long-range effect of the $hX_j^\dagger X_j$ term only. The $hX_j^\dagger X_j$ coupling is expressed in terms of m_X for convenience. It is not necessarily proportional to m_X in complete models, since we typically expect other sources for m_X besides the Higgs vacuum expectation value. Indeed, for a scalar X boson, a bare mass is allowed by all unitary symmetries. It may be forbidden by a nonunitary symmetry, such as supersymmetry, but appears as a soft supersymmetry-breaking term in the MSSM.

In this setup, if the relative mass difference $\Delta \equiv (m_X - m_\chi)/m_\chi$ is small, the DM density is determined by the χ self-annihilation, the $\chi - X$ and $\chi - X^\dagger$ coannihilation and the $X - X^\dagger$ annihilation, as we now describe.

III. RELIC ABUNDANCE

The DM density for a system of (co)annihilating particles is determined by the Boltzmann equation [2],

$$\frac{d\tilde{Y}}{dx} = -\sqrt{\frac{\pi}{45}}\frac{g_{*,\mathrm{eff}}^{1/2} M_{\mathrm{Pl}} m_\chi \langle\sigma_{\mathrm{eff}} v_{\mathrm{rel}}\rangle}{x^2}(\tilde{Y}^2 - \tilde{Y}_{\mathrm{eq}}^2), \quad (3)$$

where $\tilde{Y}$ is the sum of the yields of all coannihilating species, $\tilde{Y} = \sum_i Y_i = \sum_i n_i/s$ with $i = \chi, X, X^\dagger$. $s \equiv (2\pi^2/45)g_{*S}T^3$ is the entropy density of the Universe, $g_{*,\mathrm{eff}}$, g_{*S} are the energy and entropy degrees of freedom, and $x \equiv m_\chi/T$ is the time parameter. The yields in equilibrium are

$$Y_i^{\mathrm{eq}} = \frac{90}{(2\pi)^{7/2}}\frac{g_i}{g_{*S}}[(1+\delta_i)x]^{3/2}e^{-(1+\delta_i)x}, \quad (4)$$

with $\delta_\chi = 0$, $\delta_{X,X^\dagger} = \Delta$ and $g_\chi = 2$, $g_{X,X^\dagger} = 3$. As seen from Eq. (4), if the NLP is close in mass to the LP, its density is only mildly more suppressed, and it contributes to the DM density substantially.

The thermally averaged effective cross section includes all (co)annihilation processes weighted by the densities of the participating species. We assume that the dominant contribution is the $XX^\dagger$ annihilation cross section $\sigma_{XX^\dagger}$, such that

$$\langle\sigma_{\mathrm{eff}} v_{\mathrm{rel}}\rangle = \frac{2Y_X^{\mathrm{eq}} Y_{X^\dagger}^{\mathrm{eq}}\langle\sigma_{XX^\dagger} v_{\mathrm{rel}}\rangle}{\tilde{Y}_{\mathrm{eq}}^2}, \quad (5)$$

where v_{rel} is the relative velocity. In our model, the dominant annihilation channels are the s-wave processes $XX^\dagger \to gg, hh$. The annihilations $XX^\dagger \to q\bar{q}, gh$ are p-wave suppressed, and we neglect them for simplicity. The cross sections for the s-wave processes are

$$(\sigma v_{\mathrm{rel}})_{XX^\dagger\to gg} = \frac{14}{27}\frac{\pi\alpha_s^2}{m_X^2}\times\left(\frac{2}{7}S_0^{[\mathbf{1}]} + \frac{5}{7}S_0^{[\mathbf{8}]}\right), \quad (6a)$$

$$(\sigma v_{\mathrm{rel}})_{XX^\dagger\to hh} = \frac{4\pi\alpha_h^2}{3m_X^2}\frac{(1-m_h^2/m_X^2)^{1/2}}{[1-m_h^2/(2m_X^2)]^2}\times S_0^{[\mathbf{1}]}, \quad (6b)$$

where $\alpha_h \equiv g_h^2/(16\pi)$ [24,25] and $\alpha_s \equiv g_s^2/(4\pi)$. As seen, σv_{rel} factorize into their perturbative values and the Sommerfeld factors S_0 that encapsulate the effect of the long-range interaction, which we discuss next.

Besides the direct annihilation processes (6), the formation and decay of $X - X^\dagger$ bound states may deplete DM significantly [7,13,17,18,26–28]. Since our focus here is to demonstrate the long-range effect of the Higgs, we shall neglect these processes, which involve considerable technicalities, and present a complete treatment elsewhere [29]. Suffice to say that bound-state effects imply an even stronger impact of the Higgs exchange on the DM density.

IV. HIGGS ENHANCEMENT

If two particles couple to a light force mediator, then their long-range interaction distorts their wave packets. This is known as the Sommerfeld effect [30,31], which enhances or suppresses the inelastic scattering at low v_{rel}, for attractive or repulsive interactions, respectively.

In our model, X and $X^\dagger$ interact via the gluons and the Higgs. The long-range effect of these interactions is captured by the ladder diagrams shown in Fig. 1. The resummation of all two-particle irreducible diagrams amounts to solving the Schrödinger equation with a mixed Coulomb and Yukawa potential,

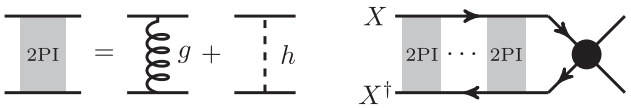

FIG. 1. The interaction of $X, X^\dagger$ at infinity affects the annihilation processes. The ladder represents the resummation of the two-particle irreducible diagrams (2PI) that yield a long-range effect: the gluon and the Higgs exchange. The black blob indicates the various annihilation channels.

$$V(r) = -\frac{\alpha_g}{r} - \frac{\alpha_h}{r} e^{-m_h r}. \tag{7}$$

The coupling α_g depends on the color representation of the $X, X^\dagger$ state. The color space decomposes as $\mathbf{3} \otimes \bar{\mathbf{3}} = \mathbf{1} \oplus \mathbf{8}$; in the singlet state, the gluon exchange is attractive with $\alpha_g = (4/3)\alpha_s$, while in the octet state, the interaction is repulsive with $\alpha_g = -\alpha_s/6$ [32].

While previous works examined the gluon exchange, we consider also the attractive force mediated by the Higgs. The Higgs exchange enhances the attraction in the singlet state, and reduces, or overcomes the repulsion in the octet state. This has not been computed before, but as we show, affects the DM density significantly.

The scattering states are described by a wave function $\phi_{\mathbf{k}}(\mathbf{r})$ that depends on $\mathbf{k} = \mu \mathbf{v}_{\rm rel}$, where $\mu = m_X/2$ is the reduced mass and $\mathbf{v}_{\rm rel}$ the relative velocity. We define the dimensionless coordinate $\mathbf{z} \equiv k\mathbf{r}$, and the parameters

$$\zeta_{g,h} \equiv \frac{\mu \alpha_{g,h}}{\mu v_{\rm rel}} = \frac{\alpha_{g,h}}{v_{\rm rel}}, \qquad d_h \equiv \frac{\mu \alpha_h}{m_h}. \tag{8}$$

Then, $\phi_{\mathbf{k}}$ is determined by the Schrödinger equation,

$$\left\{ \nabla_{\mathbf{z}}^2 + 1 + \frac{2}{z}\left[\zeta_g + \zeta_h \exp\left(-\frac{\zeta_h z}{d_h} \right) \right] \right\} \phi_{\mathbf{k}} = 0, \tag{9}$$

and the standard boundary condition at $r \to \infty$ of an incoming plane wave plus an outgoing spherical wave [33]. For s-wave annihilation, the Sommerfeld factor

$$S_0(\zeta_g, \zeta_h, d_h) \equiv |\phi_{\mathbf{k}}(0)|^2 \tag{10}$$

multiplies the perturbative cross section [34]. In Eq. (6), $S_0^{[\mathbf{1}]} = S_0[4\alpha_s/(3v_{\rm rel}), \alpha_h/v_{\rm rel}, m_X\alpha_h/(2m_h)]$ and $S_0^{[\mathbf{8}]} = S_0[-\alpha_s/(6v_{\rm rel}), \alpha_h/v_{\rm rel}, m_X\alpha_h/(2m_h)]$.

Due to the running of the strong coupling, the various factors of α_s must be evaluated at the appropriate momentum transfer Q. In the vertices of the $XX^\dagger \to gg$ tree-level diagram, $Q = m_X$ is the momentum of the radiated gluons. In the ladder diagrams that determine the Sommerfeld factors, $Q = \mu v_{\rm rel}$ is the average momentum transfer between $X, X^\dagger$. The running of α_s is implemented according to [35,36]. α_h is also subject to running that can be computed within UV complete models. Here we neglect this effect, which however is not expected to change our conclusions.

The dimensionless parameters of Eq. (8) contrast physical scales. The Bohr momentum $\mu\alpha$ indicates the momentum transfer around or below which nonperturbative effects arise; the parameters ζ_g and ζ_h compare this scale with the average momentum exchange between the interacting particles, $\mu v_{\rm rel}$. For the Yukawa term, d_h compares the Bohr radius $(\mu\alpha_h)^{-1}$ with the range of the potential, m_h^{-1}. It is typically expected that the Sommerfeld effect arises roughly for $|\zeta_g| \gtrsim \mathcal{O}(1)$ and ζ_h, $d_h \gtrsim \mathcal{O}(1)$, for the Coulomb and Yukawa potentials, respectively, and that the Coulomb limit of the Yukawa potential is attained for $d_h \gtrsim \zeta_h$ ($\mu v_{\rm rel} \gtrsim m_h$). Circumscribing this parameter range more precisely is important for anticipating the phenomenological implications of force mediators. We find that the interplay of the Coulomb and Yukawa terms affects this determination. In Figs. 2 and 3, we illustrate this point.

In Fig. 2, we explore the dependence of S_0 on d_h. We fix $\zeta_h = 0.4$; given the typical values of the velocity during freeze-out, $v_{\rm rel} \sim 0.2$, this corresponds to sizable but moderate couplings, $\alpha_h \sim 0.08$. The red line, $\zeta_g = 0$, shows the Higgs enhancement without the effect of gluon exchange. We may observe that for d_h as low as $\sim$0.2 the enhancement is substantial, $S_0 \sim 1.8$, and amounts to about half of the enhancement of the Coulomb limit. For the SM Higgs mass of 125 GeV, $d_h \sim 0.2$ is realized for moderate α_h and low enough m_X to be probed by collider experiments; for instance, $\alpha_h = 0.1$ and $m_X = 500$ GeV or $\alpha_h = 0.05$ and $m_X = 1$ TeV.

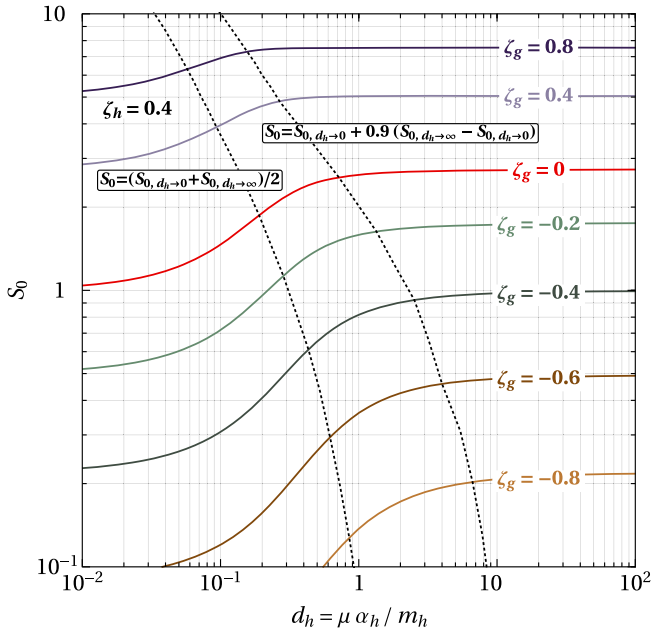

FIG. 2. The Sommerfeld factor in the mixed Coulomb and Yukawa potential of Eq. (7). At $d_h \to 0$ and ∞, the Coulomb limit is attained, $S_0 \simeq 2\pi\zeta/(1 - e^{-2\pi\zeta})$, with $\zeta = \zeta_g$ and $\zeta_g + \zeta_h$, respectively. The dotted black lines mark the d_h values for which S_0 is above its $d_h \to 0$ limit by 50% (left) and 90% (right) of the difference toward its $d_h \to \infty$ limit.

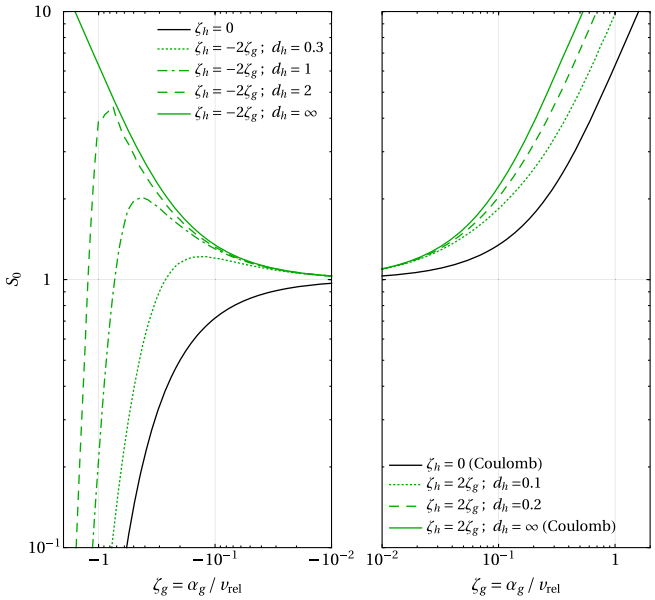

FIG. 3. S_0 vs ζ_g, for both repulsive (left panel) and attractive (right panel) Coulomb interaction. We take the Yukawa coupling to be twice as strong as the Coulomb one, $\alpha_h = 2|\alpha_g|$, and vary the parameter $d_h \equiv \mu\alpha_h/m_h$.

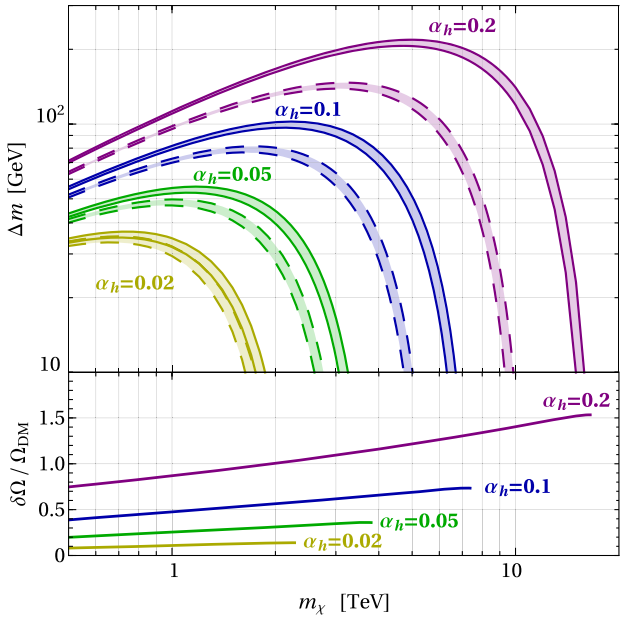

FIG. 4. Upper panel: The mass difference between the LP and the NLP vs the DM mass, for different couplings to the Higgs. The bands indicate the 3σ uncertainty on $\Omega_{\rm DM}$. The dashed lines include only the effect of gluon exchange, while the solid lines incorporate the Higgs enhancement. Lower panel: The effect of the Higgs enhancement on the DM density ranges from 10% to 150%, for the parameters considered. Δm is fixed for every $m_{\rm DM}$ and α_h, by the full freeze-out computation that includes the Higgs exchange.

Let us next consider the superposition of the Yukawa and the Coulomb potentials. The dotted black lines in Fig. 2 depict an important trend. For an attractive Coulomb term, the Yukawa contribution to S_0 is significant (with respect to its full capacity that is determined by its Coulomb limit) for even lower d_h than in the case of a pure Yukawa potential. That is, the Yukawa interaction manifests as long range for an even smaller hierarchy between scales. This feature has not been identified in DM studies before, but has a significant implication. It indicates that the Higgs enhancement is important for lower α_h and/or m_X than anticipated.

It is also striking that the Yukawa attraction can considerably ameliorate or fully overcome the suppression due to the repulsive Coulomb potential still for modest values of d_h. For this to occur, it is of course important that α_h is at least comparable to $|\alpha_g|$. In the model considered here, the Coulomb coupling in the octet state is $\alpha_g = -\alpha_s/6 \sim -0.02$, where we took $\alpha_s \sim 0.1$. It follows that even weak couplings to the Higgs can substantially enhance the annihilation rate of the octet state.

Nevertheless, the Coulomb suppression is exponential in ζ_g, and dominates over the Yukawa attraction at low $v_{\rm rel}$ (large $|\zeta_g|$), as seen in Fig. 3 (left). This does not change our earlier conclusion though, since the DM relic density is determined mostly at earlier times, when $|\zeta_g|$ is not much larger than 1.

V. IMPACT ON THE RELIC DENSITY

The above discussion suggests that the impact of the Higgs exchange on the DM density can be significant. This is indeed so. We compute the DM freeze-out with and without the Higgs enhancement and present our results in Fig. 4, for α_h in the range 0.02–0.2.[1] The enhanced annihilation rate implies that $\Omega_{\rm DM}$ is obtained for larger Δm and/or m_χ, as shown in the upper panel. Already for $\alpha_h = 0.02$, the effect exceeds the 3σ experimental uncertainty in $\Omega_{\rm DM}$, while for larger α_h it becomes very severe, as seen in the lower panel. While here we focus on $m_X \geq 500$ GeV to be on par with experimental constraints, the Higgs enhancement can affect the DM density significantly even for lower masses, as can be extrapolated from the lower panel of Fig. 4, and deduced from Figs. 2 and 3, by appropriate estimates.

In the upper panel of Fig. 5, we focus on low DM masses, $m_\chi = (0.5, 1, 2)$ TeV that can be probed at current

[1]We may estimate the value of α_h around which our computation breaks down by considering the upper bound on the inelastic cross sections implied by the S-matrix unitarity [37]. Applying the s-wave unitarity bound on Eq. (6b), we find $\alpha_h < 0.7$ (neglecting α_s). Around and above this value, higher order corrections must be considered (see Refs. [13,38] for related discussion). Note that this condition is stronger that the commonly assumed perturbativity condition $\alpha_h < 4\pi$. Depending on the UV completion of the theory, additional unitarity and perturbativity conditions may be pertinent.

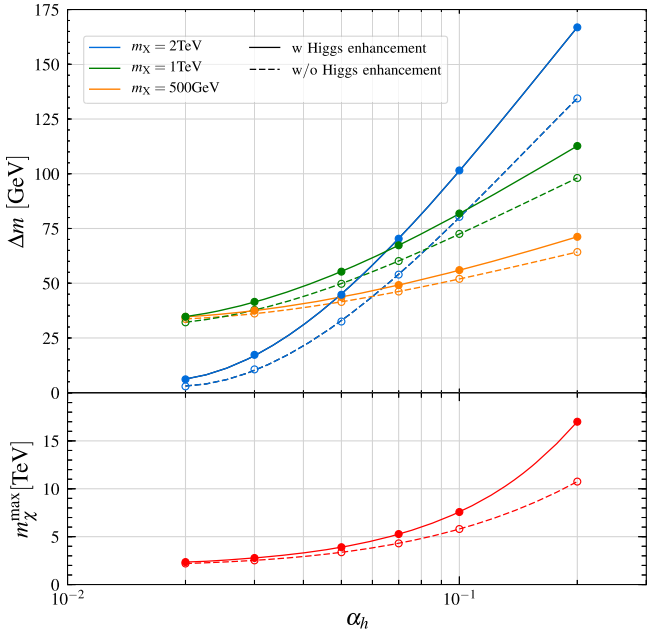

FIG. 5. The mass difference $\Delta m = m_X - m_\chi$ for $m_\chi = (0.5, 1, 2)$ TeV (upper panel), and the maximal DM mass (lower panel) versus α_h, with Higgs enhancement (solid lines) and without (dashed lines).

and future colliders, and show the considerable increase in the predicted mass gap Δm. The Higgs enhancement implies a stronger lower limit on Δm for a given m_χ and α_h; additional (co)annihilation channels—potentially also Higgs-enhanced—that are expected in complete models, shift the prediction for Δm to higher values.

The maximum DM mass $m_\chi^{\max}$ in agreement with $\Omega_{\rm DM}$ is shown in the lower panel of Fig. 5. The Higgs enhancement shifts $m_\chi^{\max}$ substantially, by about 150 GeV for $\alpha_h = 0.02$, to more than 6 TeV for $\alpha_h = 0.2$.

The mass gap and the maximum DM mass have important experimental implications, as we discuss below.

VI. HIGGS ENHANCEMENT IN THE MSSM

Sizable couplings to the Higgs occur in the MSSM, especially in light stop scenarios with maximal mixing between stop mass eigenstates, that are motivated by the value of the Higgs mass [3,20]. In the MSSM11, we have identified an example scenario of neutralino LP and stop NLP, with masses $m_{\tilde\chi_1^0} = 982.5$ GeV and $m_{\tilde t_1} = 1066.1$ GeV, where the coupling to the Higgs amounts to $\alpha_h \simeq 0.15$. The MSSM parameters are (dimensionful quantities in GeV) $\tan\beta = 16.3$, $\mu = 2653.1$, $m_{A^0} = 1917.9$, $M_1 = 972.1$, $M_2 = 1944.1$, $M_3 = 5832.4$, $M_{\tilde q_{1,2}} = 3054.3$, $M_{\tilde q_3} = 2143.7$, $M_{\tilde\ell} = 2248.3$, $M_{\tilde u_3} = 2143.7$, and $A_t = -4380.93$. As large trilinear couplings are known to give rise to color-breaking minima in the scalar potential that could endanger the stability of the $SU(3)_c$-symmetric vacuum, we have checked with `Vevacious` [39,40] for stability. We found that in this scenario, the color-symmetric vacuum is metastable but sufficiently long-lived. Thermal corrections imply an upper limit on the reheating temperature of $T \approx M_{\rm SUSY}$. In scenario B of Ref. [4], with $m_{\tilde\chi_1^0} = 1306.3$ GeV and $m_{\tilde t_1} = 1363.0$ GeV, we find $\alpha_h = 0.03$. Moreover, in the parameter space recently explored in Ref. [10], we estimate α_h to be in the range $\sim(0.02$–$0.07)$ for $m_{\tilde t_1} = 500$ GeV and $\sim(0.01 - 0.05)$ for $m_{\tilde t_1} = 1500$ GeV. Larger couplings to the Higgs than those mentioned above may be viable, however a proper study of the vacuum stability has to be pursued for specific scenarios. Furthermore, it has been argued that large couplings of colored particles to the Higgs may lead to a new phase in the MSSM, where the standard treatment does not apply [41].

Clearly, substantial couplings to the Higgs appear in realistic models. While the Higgs enhancement has been neglected in previous studies, it is essential for interpreting the experimental results correctly.

VII. FURTHER EXPERIMENTAL IMPLICATIONS

Small mass gaps Δm that are a feature of the scenarios considered here, lead to the production of soft jets from the decay of the NLP that are difficult to probe at the LHC. The Higgs enhancement implies larger mass gaps for a given DM mass (cf. Fig. 5), therefore harder jets that may pass the detection threshold. This is important for mono-/multi-jet plus missing energy searches. Higgs-enhanced bound-state processes increase Δm further [29]. Moreover, the Higgs enhancement implies that WIMP DM may be heavier than anticipated, and motivates indirect searches in the multi-TeV regime.[2] Of course, to fully assess the experimental implications of the Higgs enhancement, proper analyses of realistic scenarios are necessary.[3]

VIII. CONCLUSIONS

We have demonstrated that the Higgs enhancement can affect the DM density significantly, thereby altering the interpretation of the experimental results within specific theories, but also motivating extended searches. Importantly, the interplay between the Higgs and other mediators—within or beyond the SM—affects the efficiency of the Higgs enhancement. Besides the scenarios considered here, we expect that the Higgs enhancement is important in a variety of models around or above the TeV

[2]Indirect signals arise from the DM self-annihilations only. In our analysis, we assumed for simplicity that they are negligible with respect to coannihilations and/or self-annihilations of the DM coannihilating partner. However, self-annihilations are expected to occur in complete models, and yield significant indirect signals.

[3]An even stronger coupling of colored particles to the Higgs than considered here, may have implications for the electroweak symmetry breaking [42,43] and colliders [42–44].

scale, including WIMP scenarios, such as the inert doublet model [18,45–49], as well as Higgs portal models (see [50] and references therein).

ACKNOWLEDGMENTS

We thank Florian Staub for providing help with `Vevacious`, and Andreas Goudelis for useful discussions. J. H. was supported by the Labex ILP (No. ANR-10-LABX-63) part of the Idex SUPER and received financial state aid managed by the Agence Nationale de la Recherche, as part of the program Investissements d'avenir (No. ANR-11-IDEX-0004-02). K. P. was supported by the ANR ACHN 2015 grant ("TheIntricateDark" project), and by the NWO Vidi grant, "Self-interacting asymmetric dark matter."

[1] P. A. R. Ade *et al.* (Planck Collaboration), Astron. Astrophys. **594**, A13 (2016).
[2] J. Edsjo and P. Gondolo, Phys. Rev. D **56**, 1879 (1997).
[3] J. Harz, B. Herrmann, M. Klasen, K. Kovarik, and Q. L. Boulc'h, Phys. Rev. D **87**, 054031 (2013).
[4] J. Harz, B. Herrmann, M. Klasen, K. Kovarik, and M. Meinecke, Phys. Rev. D **91**, 034012 (2015).
[5] J. Harz, B. Herrmann, M. Klasen, and K. Kovarik, Phys. Rev. D **91**, 034028 (2015).
[6] M. J. Baker *et al.*, J. High Energy Phys. 12 (2015) 120.
[7] J. Ellis, F. Luo, and K. A. Olive, J. High Energy Phys. 09 (2015) 127.
[8] J. Harz, B. Herrmann, M. Klasen, K. Kovarik, and P. Steppeler, Phys. Rev. D **93**, 114023 (2016).
[9] J. Ellis, J. L. Evans, F. Luo, and K. A. Olive, J. High Energy Phys. 02 (2016) 071.
[10] A. Pierce, N. R. Shah, and S. Vogl, Phys. Rev. D **97**, 023008 (2018).
[11] J. Hisano, S. Matsumoto, and M. M. Nojiri, Phys. Rev. D **67**, 075014 (2003).
[12] J. Hisano, S. Matsumoto, and M. M. Nojiri, Phys. Rev. Lett. **92**, 031303 (2004).
[13] B. von Harling and K. Petraki, J. Cosmol. Astropart. Phys. 12 (2014) 033.
[14] A. Hryczuk, Phys. Lett. B **699**, 271 (2011).
[15] M. Cirelli, T. Hambye, P. Panci, F. Sala, and M. Taoso, J. Cosmol. Astropart. Phys. 10 (2015) 026.
[16] M. Beneke, A. Bharucha, F. Dighera, C. Hellmann, A. Hryczuk, S. Recksiegel, and P. Ruiz-Femenia, J. High Energy Phys. 03 (2016) 119.
[17] S. P. Liew and F. Luo, J. High Energy Phys. 02 (2017) 091.
[18] S. Biondini and M. Laine, J. High Energy Phys. 08 (2017) 047.
[19] L. Lopez-Honorez, T. Schwetz, and J. Zupan, Phys. Lett. B **716**, 179 (2012).
[20] H. E. Haber and R. Hempfling, Phys. Rev. Lett. **66**, 1815 (1991).
[21] H. E. Haber, R. Hempfling, and A. H. Hoang, Z. Phys. **C75**, 539 (1997).
[22] W.-Y. Keung, I. Low, and Y. Zhang, Phys. Rev. D **96**, 015008 (2017).
[23] A. Ibarra, A. Pierce, N. R. Shah, and S. Vogl, Phys. Rev. D **91**, 095018 (2015).
[24] K. Petraki, M. Postma, and M. Wiechers, J. High Energy Phys. 06 (2015) 128.
[25] K. Petraki, M. Postma, and J. de Vries, J. High Energy Phys. 04 (2017) 077.
[26] S. Kim and M. Laine, J. High Energy Phys. 07 (2016) 143.
[27] S. Kim and M. Laine, J. Cosmol. Astropart. Phys. 01 (2017) 013.
[28] S. El Hedri, A. Kaminska, M. de Vries, and J. Zurita, J. High Energy Phys. 04 (2017) 118.
[29] J. Harz and K. Petraki (to be published).
[30] A. D. Sakharov, Soviet Physics Uspekhi **34**, 375 (1991).
[31] A. Sommerfeld, Ann. Phys. (Berlin) **403**, 257 (1931).
[32] Y. Kats and M. D. Schwartz, J. High Energy Phys. 04 (2010) 016.
[33] J. J. Sakurai, *Modern quantum mechanics* (Addison-Wesley, Reading, MA, 1993).
[34] S. Cassel, J. Phys. G **37**, 105009 (2010).
[35] C. Patrignani *et al.* (Particle Data Group), Chin. Phys. C **40**, 100001 (2016).
[36] G. M. Prosperi, M. Raciti, and C. Simolo, Prog. Part. Nucl. Phys. **58**, 387 (2007).
[37] K. Griest and M. Kamionkowski, Phys. Rev. Lett. **64**, 615 (1990).
[38] I. Baldes and K. Petraki, J. Cosmol. Astropart. Phys. 09 (2017) 028.
[39] J. E. Camargo-Molina, B. O'Leary, W. Porod, and F. Staub, Eur. Phys. J. C **73**, 2588 (2013).
[40] J. E. Camargo-Molina, B. Garbrecht, B. O'Leary, W. Porod, and F. Staub, Phys. Lett. B **737**, 156 (2014).
[41] G. F. Giudice and A. Kusenko, Phys. Lett. B **439**, 55 (1998).
[42] J. M. Cornwall, A. Kusenko, L. Pearce, and R. D. Peccei, Phys. Lett. B **718**, 951 (2013).
[43] L. Pearce, A. Kusenko, and R. D. Peccei, Phys. Rev. D **88**, 075011 (2013).
[44] Z. Kang, Phys. Lett. B **771**, 313 (2017).
[45] R. Barbieri, L. J. Hall, and V. S. Rychkov, Phys. Rev. D **74**, 015007 (2006).
[46] L. Lopez Honorez, E. Nezri, J. F. Oliver, and M. H. G. Tytgat, J. Cosmol. Astropart. Phys. 02 (2007) 028.
[47] T. Hambye, F. S. Ling, L. Lopez Honorez, and J. Rocher, J. High Energy Phys. 07 (2009) 090; 05 (2010) 066.
[48] A. Goudelis, B. Herrmann, and O. Stal, J. High Energy Phys. 09 (2013) 106.
[49] B. Eiteneuer, A. Goudelis, and J. Heisig, Eur. Phys. J. C **77**, 624 (2017).
[50] K. Assamagan *et al.*, arXiv:1604.05324.